Design of a Micro-Class Aircraft for the SAE AeroEast Heavy Lift Competition 2012

A Major Qualifying Project Report
submitted to the Faculty
of the

WORCESTER POLYTECHNIC INSTITUTE

In partial fulfillment of the requirements for the
Degree of Bachelor of Science
by

Steven Andrews

Benjamin Grossman-Ponemon

Shauna-Marie Hendricks

Geoffrey Hong

Christopher McKenzie

Kyle Morette

Date: May 1, 2012

Professor Simon Evans, Advisor

Professor David J. Olinger, Co-Advisor

Abstract:

The goal of this MQP was to design, construct, and fly a remote control aircraft for the 2012 SAE Aero East Heavy Lift Competition, Micro Class. The SAE competition restricted the size, weight and launch method of the aircraft. The aircraft must disassemble to fit in a 24”×18”×8” box, be assembled by a team of two in three minutes, and complete a circuit carrying its payload. To remain competitive, the aircraft needed to maintain a high payload percentage, be simple to construct, stable at different weights, and durable. General aircraft parameters were selected through the aircraft design process. The detailed design of the aircraft was conducted using computer aided design software, and then the parts were manufactured from balsa wood using the laser-cutting machine. Throughout the design process, wind tunnel tests were performed on scaled models fabricated by the rapid prototype machine. Ultimately, a flightworthy aircraft was constructed that met competition requirements. Future tests will confirm aircraft design analysis.

Acknowledgements:

We would like to thank our project advisors, Professor David Olinger and Professor Simon Evans for their assistance and guidance over the course of the project. We would also like to thank Pam St. Louis in the Mechanical Engineering department and Alan Hutchinson for all of their help.

Authorship Page

Abstract: All

Acknowledgements: Morette

Nomenclature All

Executive Summary: Morette

1. Introduction: Hong

2. Design Process: McKenzie, Hendricks

3. Calculations
    - 3.2 Weight Build-Up/Analysis: Hong
    - 3.3 Airfoil Selection and Wing and Tail Sizing: Hendricks, Grossman-Ponemon
    - 3.4 Wing and Tail Aerodynamic Properties: Hendricks, Grossman-Ponemon
    - 3.5 Propulsion: Morette
    - 3.6 Performance: Grossman-Ponemon
    - 3.7 Aircraft Stability and Control: Andrews
    - 3.8 Structural Analysis: Grossman-Ponemon

4. Innovations: Hendricks,McKenzie

5. Construction
    - Construction Process: Andrews
    - Mylar Guide: Hendricks

6. Results: Grossman-Ponemon, McKenzie, Morette

7. Conclusions: Hong, Hendricks

8. Recommendations: Hong

Table of Contents

List of Figures

List of Tables

Nomenclature

A_{max}	Maximum Cross-section Area
A_{prop}	Prop Area
AR	Aspect Ratio
b	Span
$\bar{c}$	Mean Aerodynamic Chord
c	Chord
c_{root}	Root Chord
$C_{dinduced}$	Induced Drag Coefficient
C_{dmin}	Minimum Drag Coefficient
C_{d0}	Parasitic Drag Coefficient
C_D	Drag Coefficient
$C_{f,c}$	Skin Friction Coefficient of Component c
$C_{f,lam}$	Laminar Skin Friction Coefficient
$C_{f,turb}$	Turbulent Skin Friction Coefficient
$C_{m,hinge}$	Hinge Moment Coefficient
$C_{m,LE}$	Leading Edge Moment Coefficient
$C_{m,c/4}$	Quarter Chord Moment Coefficient
C_n	2D Normal Force Coefficient
C_N	3D Normal Force Coefficient
C_l	2D Coefficient of Lift
$Cl_{\alpha w}$	Lift Curve Slope of Wing
$Cl_{\alpha h}$	Lift Curve Slope of Horizontal Tail
$C_{l,mind}$	Lift Coefficient at Minimum Drag
CG	Center of Gravity
D	Drag Force
$\frac{d\alpha_H}{d\alpha}$	Horizontal Tail Downwash Derivative
D_{prop}	Propeller Drag Force
D_{total}	Total Drag Force
$D_{induced,wing}$	Induced Drag Force of Wing
$D_{induced,HT}$	Induced Drag Force of Horizontal Tail
D_0	Parasitic Drag Force
$D_{featheredprop}$	Feathered Propeller Drag Force
e	Oswald Efficiency Factor
f	Slenderness Factor
F	Body Lifting Factor
FF_c	Form Factor of Component c
g	Gravitational Acceleration
H_{total}	Total Hinge Moment
$H_{aerodynamic}$	Aerodynamic Hinge Moment
H_{weight}	Hinge Moment due to Weight
HT	Horizontal Tail
I	Current
I_{zz}	Moment of Inertia

k_v	Motor RPM to Voltage Rating
L	Lift Force
M	Mach number, Bending Moment
n_{blades}	Number of Blades
q	Dynamic Pressure
P	Power
Q_c	Interference Factor of Component c
Re	Reynolds Number
S	Wing Planform Area
$S_{control}$	Control Surface Area
S_{exp}	Exposed Wing Area
S_h	Horizontal Tail Area
$S_{wet,c}$	Wetted Surface Area of Component c
S_{ref}	Reference Area (Wing Planform Area)
r	Radius
R	Universal Gas Constant
T	Thrust
(t/c)	Thickness Ratio
Temp	Temperature
v	Velocity
V	Voltage
V_{batt}	Battery Voltage
V_{pitch}	Pitch Speed
VT	Vertical Tail
y	Vertical Distance from Neutral Axis of Spar Cross Section
W	Weight
x_{cg}	Center of Gravity Location from Nose of Plane
$x_{cg,s}$	Center of Gravity of Control Surface from Hinge
x_{ac}	Location of Aerodynamic Center from Nose
$(x/c)_m$	Chordwise Position of Max Thickness
$\bar{x}_{acw}$	Normalized Aerodynamic Center Location of Wing
$\bar{x}_{np}$	Normalized Neutral Point Location
$\bar{x}_{mf}$	Normalized Most Forward Point Location
$\bar{x}_{ach}$	Normalized Aerodynamic Center Location of Tail
λ	Taper Ratio
Λ_m	Sweep Angle at Max Thickness of Chord
Λ_{LE}	Sweep Angle of Leading Edge
α	Angle of Attack
β	Mach Compression Factor
γ	Specific Heat Ratio
μ	Dynamic Viscosity/Coefficient of Friction
η	Ratio of 2D Lift Curve Slope to Theoretical Slope
η_h	Tail Efficiency Factor

η_{prop}	Propeller Efficiency
ρ	Density
σ_{max}	Max Bending Stress

Executive Summary

Each year, SAE International hosts a competition to design, construct, and fly various types of remote controlled aircraft. This Major Qualifying Project focused on the creation of a heavy lift micro-class aircraft to fly in the SAE Aero Design East 2012 competition. The project duration is three terms long consisting of a design phase, a build phase, and a testing phase. Each phase takes roughly a term each, ending with the competition on April 27th, 28th, and 29th. The goal of this MQP is to create a micro-class aircraft that successfully flies, conforms to all the competitions design criteria, and is of the lightest possible weight while carrying the heaviest payload possible. The secondary goal of the design is to place competitively in the SAE Aero Design East competition. The airplane design has to conform to rules which limit overall plane dimensions, construction materials and launching options (either hand launch or elastic device launch), and prohibit lighter-than-air. The cargo bay used to carry the payload must be able to fit a 2" x 2" x 5" payload. Aside from this however, the restrictions mainly focused on each team's ability to design an aerodynamically sound aircraft with heavy lift capabilities.

WPI has limited experience in the SAE Aero Design competition. Only two MQP teams have participated in the competition in recent years, competing in the regular class. The 1998-1999 MQP showed strong results in the Design Report and Presentation sections of the competition. However, due to the inability to fly the plane, the team was unable to qualify for a competitive standing amongst the other teams. The 1997-1998 team had the most success by qualifying for the competition; the first to do so from WPI. However, due to catastrophic wing spar failure, the team was only capable of lifting a payload weight of twelve pounds.

Similar to previous MQP project groups, our team split up into smaller subgroups consisting of propulsion analysis, stability analysis and aerodynamic design. Due to the large

lapse in time between the previous SAE Aero East competition MQP and this team's MQP as well as a moderate difference in rules (including a change in class size), the team chose to start anew with the design. As such, priorities in design were taken based on the competition. The competition has three parts: a flight competition, a technical presentation and a design report.

The design of the aircraft followed the structure of the ME 4770 course. As such, initial weight estimation led to airfoil selection and wing dimensions. These parameters were used to generate aerodynamic values such as lift, drag, and flight velocity. Stability and propulsion analysis were performed to determine necessary electronics requirements and their placement in the aircraft. Modifications to these initial parameters were performed over five iterations.

The general structural layout of the plane was a conventional tail design and high wing configuration. This allowed the aircraft four separate control surfaces for better flight control: two ailerons, rudder, and elevator. Due to the structural loads of the plane, the building materials (balsa wood, carbon fiber spars) were determined and included in the construction process instructions. SolidWorks was used extensively to design the aircraft to allow for easy modification of the design.

With the design finalized, the wooden frame of the plane was constructed with parts manufactured using the laser cutter. This process proved to be effective as it didn't take money from the budget and allowed for quick turn-around on multiple plane constructions. The structure was assembled using quick-dry super glue, and then covered in Mylar to create the outer surfaces of the plane.

The electronics of the plane were modified to all have the same connectors. The wires for the electronics were also trimmed or extended to appropriate lengths as dictated by the electronics placement.

Unpowered versions of the aircraft were constructed first to perform glide and wing break tests. After testing, a fully working aircraft was constructed. Flight tests were attempted, and successful empty weight flights were achieved. With the addition of payload, the aircraft was not able to successfully fly. It was later discovered that the motor was underpowered to achieve necessary thrust values.

Due to the evolving nature of the aircraft and the many lessons learned throughout the design process, this report contains many recommendations to assist future teams in their endeavors.

1. Introduction

1.1 Background

The Society of Automotive Engineers' (SAE) Aero Design competition is an annual competition held to provide undergraduate and graduate engineering students a real-life engineering challenge [1]. The competition is split into three different classes: regular, advanced, and micro. Each class has its own list of specifications with which the teams' design must comply. Each team is tasked with designing a fully operational aircraft with the goal of maximizing the aircraft's payload while minimizing the aircraft's empty weight. To prove the aircraft's air-worthiness it must take off, complete a circuit around the airfield, and land intact.

To best achieve the task of the micro-class competition, the aircraft designed by this team utilized a conventional aircraft configuration, which was modified to excel at providing heavy lift capabilities. The conventional aircraft configuration was chosen over more advanced designs because of its performance predictability. Our group decided it would be more beneficial to utilize a standard design rather than a radically different aircraft because of the limitations of the competition and the challenges that might arise along the design process.

In the following sections, we outline the design process used to create our micro aircraft. We begin with a broad view of the design process with which we selected individual components and how those components were altered as we adapted our design throughout five iterations. Calculations used to justify the aerodynamic, propulsion, and stability performance are detailed and a final weight build-up is given. Finally, we list new innovations utilized in the design and analysis of our final aircraft.

1.2 Problem Statement and Objectives

The team's objectives for this design project were:

1. Design and fabrication of a heavy-lift radio-controlled (RC) aircraft which met the requirements to compete in the Micro Class in the 2012 SAE Aero East Design Competition.

Major design requirements set by the SAE Aero competition rules and guidelines [2] included:

1. The aircraft must take-off; complete a circuit around the air field, and land.
2. The aircraft must maintain structural integrity throughout the duration of its flights.

Important rules specific to the Micro Class included:

1. The aircraft cannot be a lighter-than-air or rotary wing aircraft.
2. The aircraft must possess an empty weight of less than 2 lbs.
3. The aircraft must operate on an electric motor.
4. The aircraft must be launched by hand or with the use of an elastic launching device.
5. The aircraft and all components essential to its operation must fit within a 24" x 18" x 8" box.
6. The aircraft must be able to accommodate a 2" x 2" x 5" block representing the payload.
7. The aircraft must be flight-worthy without carrying a payload.
8. The aircraft must be able to be constructed (to fly-ready conditions) in under 3 minutes.

2. Design Process

The primary reference sources for the design stages of the project consisted of aircraft design and aerodynamics textbooks, course notes, and some stability references. We also referenced information on past winners on the SAE website and the associated data. Our design steps are outlined in the following flow diagram.

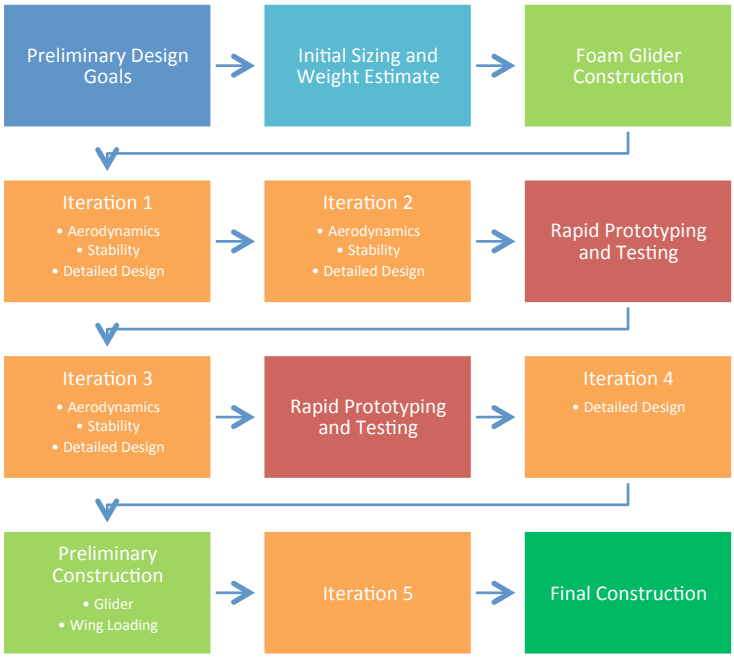

Figure 2.1 Design Flow Diagram

2.1 Aircraft Design Approach

The group primarily used two aircraft design references. The first reference was notes from WPI's ME4770 Aircraft Design course, provided by Professor David J. Olinger (WPI) [3]. These student oriented notes outlined the design processes of an aircraft based on mission statement and flight parameters. Daniel Raymer's *Aircraft Design: A Conceptual Approach* [4] contained similar information to the class notes, but in greater detail. Combining both materials resulted in a more thorough design process. Ultimately, our design goal was to design an aircraft

that would sustain controlled flight. Once the basic requirements of flight were achieved, we focused on making the aircraft more efficient.

We also made use of past competition designs and results. Our major design parameters included the payload fraction, payload capacity, and empty weight of previous top placing teams from both Aero East and Aero West competitions. It was noted that previous competitors achieved payload fractions of around 0.75 to 0.85 with Cincinnati's winning payload fraction being 0.811 [5]. Using payload fractions and total scores, we found that Cincinnati carried approximately 16 N payload with an empty weight of 3.1 N. We deemed these values competitive and made it our goal to meet or exceed these payload fractions.

2.2 Concept and Analysis

Wing: Primary concerns in the design of the wing were size, lifting capacity, wing loading, ease-of-design and construction, and drag effects. Based on the size of the aircraft and the speeds at which it would fly, we assumed that a high lift, low Reynolds number airfoil would be best suited for the competition. The ideal planform of a wing for minimum induced drag is the elliptical planform [4]. An elliptical wing is very difficult to construct; a tapered wing, however, has similar drag advantages while being far simpler to construct. The straight lines in a tapered wing mean that it is easily constructed using balsa and glue. After establishing a desired lifting capacity, in an attempt to be competitive with the 2011 Micro Class winner, and understanding the size limitations of the carrying case, we set the taper ratio and wing span of the wing. This process was repeated during each iteration of the design phase.

Tail: The primary concern when designing the tail was its ability to contribute to the stability of the aircraft. This meant that the tail, for a given moment arm, had to provide enough moment to counteract moments due to the wing-body combination, and the payload being

located away from the aircraft's center of gravity. A secondary concern related to the empennage design. We decided to place the tail at approximately the same height as the wing based on observation in previous competition designs. From the Stevens Institute of Technology micro-class report [6], the T, V, and crucifix designs each have their uses and benefits but the simplicity of designing, controlling and manufacturing a fuselage mounted tail led us to select it.

Body/Empennage: The main purpose of the body/empennage is to contain the payload and electronics of the aircraft, and to provide a moment arm for the tail in order to maintain stability. Our design constraint was the size of the carrying case and internal capacity requirements. We considered two main choices: a body with a boom-tail and a body with a space-frame empennage. The boom-tail design has the advantage of being two parts which allows for a larger tail moment arm and being lightweight. A longer empennage enhances the tail's effect on stability and more easily controls the location of the neutral point. On the other hand, with the space-frame design we would not have to attach the tail during assembly and we could use traditional materials and manufacturing methods including laser-cut balsa.

2.3 Final Aircraft Design

2.3.1 Preliminary Design

Our aircraft was designed over five iteration phases. Each iteration represents modifications due to design parameter changes or structural changes. The following are preliminary design choices made during the first two iterations of the aircraft.

The S1223 airfoil was chosen based on Selig's report for the airfoil [7]. We included a ten degree polyhedral for stability. Normally, a two degree dihedral is recommended for high, un-swept wings [4]; however, because the polyhedral would be affecting a smaller wing area, we decided to increase the angle. Our wing spar was made of carbon fiber. Carbon fiber has higher

yield strength than balsa and other woods, critical to withstanding the loading on the wing. The flight speed was increased to 11 m/s. This number was based off of the Stevens Institute of Technology's aircraft flight speed [6].

Tail: We established our tail to be a rectangular planform with NACA 0012 airfoil. The angle of attack on the tail was set at zero degrees throughout the design process. These two design selections helped to simplify later aerodynamic and stability calculations.

Body and Empennage: Early in the design process we chose to use a space-frame design. A space-frame design allowed servos to be placed in the empennage, which would have otherwise been impossible with a tail and boom design. We also chose to have the tail at approximately the same height as the wing for simpler construction. We considered semi-monocoque and monocoque designs, but ultimately chose a space frame design because of the difficulty in manufacturing thin foam structures and ease of construction using CAD.

2.3.2 Iteration Changes

Iterations 1 and 2 were basic design iterations, made in an attempt to achieve design objectives with only the smallest concern put on detailed design. By the end of Iteration 2, all major aerodynamics and stability calculations had been made. The following are detailed design changes made in later iterations.

Iteration 3: This iteration's major distinguishing factor was its three-part wing. Initially this was designed to ease construction at competition. Instead of having to connect aileron servo control wires from the wing to the receiver, the servo would be installed on a fixed central wing portion. The three-part wing also addressed the issue of stresses at the center of the carbon fiber spar. By having one spar instead of two, we were assured that the maximum shear stress of the central spar was as high as possible. During this iteration, SolidWorks drafting became increasingly detailed, with for more emphasis placed on methods of construction of the plane.

Iteration 4: In Iteration 4 a two-part wing addressed the issue of attaching the wing-tip portions to the fixed central wing. The wing-tip central spars and ribs, all being made out of wood, were found to be too soft to securely pin or attach to the central wing. The central spar, however, was made out of carbon fiber, and was more easily manipulated and stronger than the wing-tip joint. We also had more flexibility to add support to the body to accommodate the change in attachment points. Both iteration 3 and 4 made extensive use of laser cut panels to ease construction and provide structure to the aircraft

Iteration 5: Flight tests of Iteration 4 designs revealed that while the panel method made for a simpler and lighter construction, failure along the grain of $1/8^{th}$ inch panels was a significant problem, both during construction and during flight—particularly during gusts of wind. To deal with this problem the body was redesigned using ribs and longerons. This technique not only made the body stronger, but also catered to the placement of electronics and payload. Specifically designed cutouts for each electronic component and the wires were made in the ribs to aid construction. With this redesign however, also came an increase in body weight. This was deemed acceptable in order to make a flightworthy aircraft. The slightly bulkier design required a slightly increased tail span—though tail area was maintained. In addition, the new placement of electronics meant a slight change in the location of the wing to provide acceptable neutral and most forward points.

3. Aircraft Design

After deciding on the general configuration we wanted our aircraft to have we performed calculations to refine estimated numbers and create a more favorable design.

3.1 Final Aircraft Design Parameters

Based on the design process and considerations detailed above and in following sections, we arrived at the following parameters for our aircraft.

Table 3.1 Aircraft Dimensions

Structural Component	Dimension
Total Length	63.10 cm
Fuselage Length	26.00 cm
Empennage Length	26.30 cm
HT Chord	9.00 cm
HT Span	28.63 cm
HT Area	0.026 m^2
VT Chord	9.00 cm
VT Span	9.00 cm
VT Area	0.010 m^2
Wing Span	114.00 cm
Wing Chord	14.17cm
Wing Area	0.147 m^2

Table 3.2 Ambient Conditions

Ambient Conditions	
Flight Speed	11 m/s
Air Density at Sea Level	1.17 kg/m^3
Air Pressure at Sea Level	1 atm
Sea Level Temperature	26.8^0 C

3.2 Weight Build-Up/Analysis

Table 3.3 Aircraft Weight Build-up

Part	Weight (lb)
Aircraft Skeleton	1.139 N
Motor	0.423 N
Prop	0.147 N
Battery	0.774 N
Receiver/Transmitter	0.089 N
Servos: Aileron (2)	0.182 N
Servos: Elevator (2)	0.182 N
Electronic Speed Cont.	0.472 N
Total	3.772 N

Table 3.1 details the weight build-up of our aircraft. It is evident that the required electronics compose the majority of our total weight. This was where we tried to cut as much unnecessary weight as possible. We looked at several different options for each electronic component, and chose the option which had the minimal weight for the specifications we required. Our second concern was the material with which we would be constructing the aircraft structure. We looked primarily at balsa wood and basswood. They are two of the most commonly used materials in model aviation because of their densities and strength. We chose balsa wood over basswood for the majority of the structure because of its lower density (128.15 kg/m^3 vs. 448.52 kg/m^3) but implemented basswood rods in structurally critical positions for its strength (60 MPa psi vs. 15.5 MPa). A carbon fiber rod was used for the spar of the wing for its extremely high strength where basswood would not have been sufficient.

3.3 Airfoil Selection and Wing and Tail Sizing

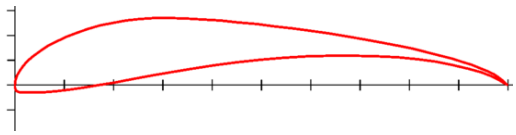

Figure 3.1 S1223 Airfoil [8]

In order to confirm that the S1223 was the best airfoil for our application, we researched numerical data for the S1223 and compared it with data available for other airfoils. The primary reference for our final selection was Selig's paper on the S1223, which showed its superiority in comparison with other heavy lift airfoils [7]. We also referenced World of Krauss for low Reynolds number data [5].

To size the wing, XFOIL was used in an iterative fashion. Using the defined airspeed and calculating density from the ideal gas law from assumed ambient temperature and pressure, we found the dynamic pressure of the system. We used inviscid flow analysis in XFOIL to find an initial lift coefficient. We then found the planform area of the wing using equation 3.1.

$$S = \frac{L}{\frac{1}{2}\rho v^2 C_l} \tag{3.1}$$

Using the taper of the wing, the defined span, and equation 3.2 [4], we found the root chord of the wing.

$$c_{root} = \frac{2S}{b(1+\lambda)} \tag{3.2}$$

Using equation 3.3 [4], we found the mean aerodynamic chord of the wing and computed the Reynolds number of the flow using equation 3.4.

$$\bar{c} = \frac{2(1+\lambda+\lambda^2)}{3(1+\lambda)} c_{root} \tag{3.3}$$

$$\mathrm{Re} = \frac{\rho v \bar{c}}{\mu} \tag{3.4}$$

Using the computed Reynolds number in XFOIL's viscous analysis, the process was repeated: we found a lift coefficient, a planform area, a root chord, a mean aerodynamic chord, and then a new Reynolds number. This process was repeated until the values converged. Table 3.4 shows the final converged values:

Table 3.4 Wing Dimensions

Reynolds Number	92534
Lift Coefficient	1.5056
Planform Area	0.147 m^2
Root Chord	19.08 cm
Mean Aerodynamic Chord	14.17 cm
Aspect Ratio	8.24

The horizontal tail was sized with a chord length of 9.00 cm and a span of 17.00 cm in an attempt to meet recommended tail volume coefficient of Raymer [4]. To achieve the desired stability margin, our tail volume coefficient ended up as .402. The limiting factors in tail sizing were the size of the box and an aspect ratio of three. The vertical tail was sized with the same chord and an aspect ratio of one.

3.4 Wing and Tail Aerodynamic Properties

We established the lift curve slope of the wing by using the Lift Coefficient equation 3.5 [4].

$$C_{L_\alpha} = \frac{2\pi(AR)}{2 + \sqrt{4 + \frac{(AR)^2 \beta^2}{\eta^2}\left(1 + \frac{\tan^2 \Lambda_{LE}}{\beta^2}\right)}}\left(\frac{S_{\exp}}{S_{ref}}\right)(F)$$

$$\beta^2 = 1 - M^2 \tag{3.5}$$

$$\eta = \frac{C_{l_\alpha}}{(2\pi/\beta)}$$

$$F = 1.07(1 + d/b)^2$$

WINGSPAN	114 cm
HEIGHT	18.7 cm
LENGTH	63.1 cm
WING AREA	f
ENGINE	eRC 400 Brushless
EMPTY WEIGHT	1 lbf

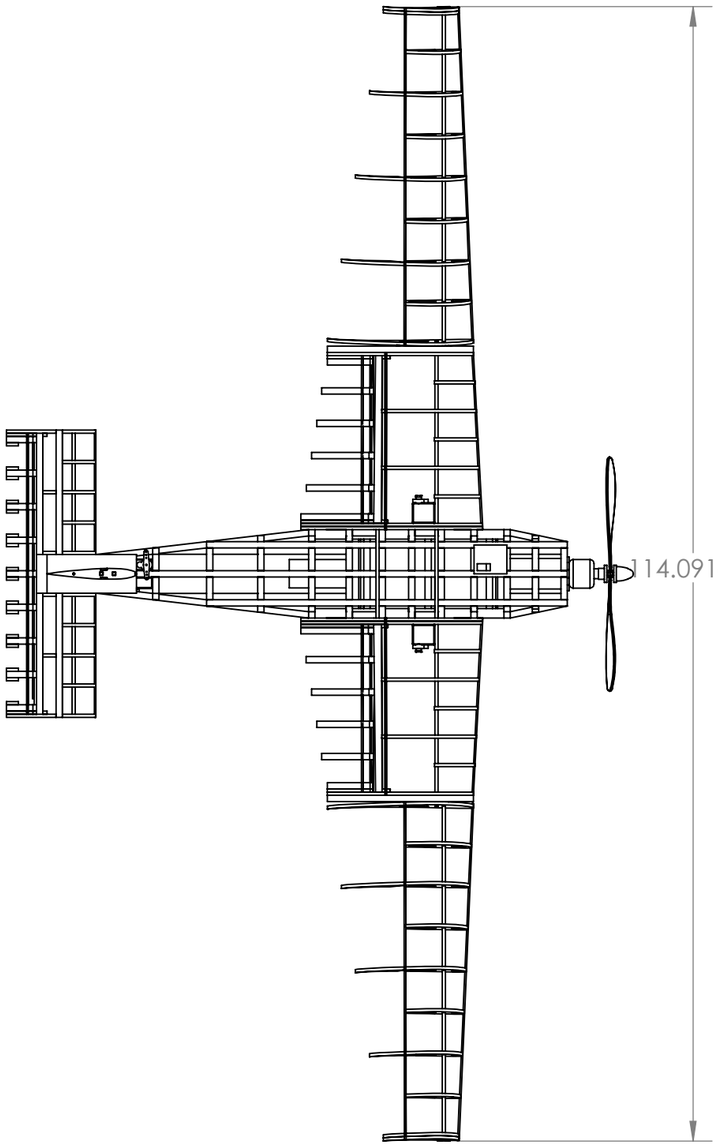

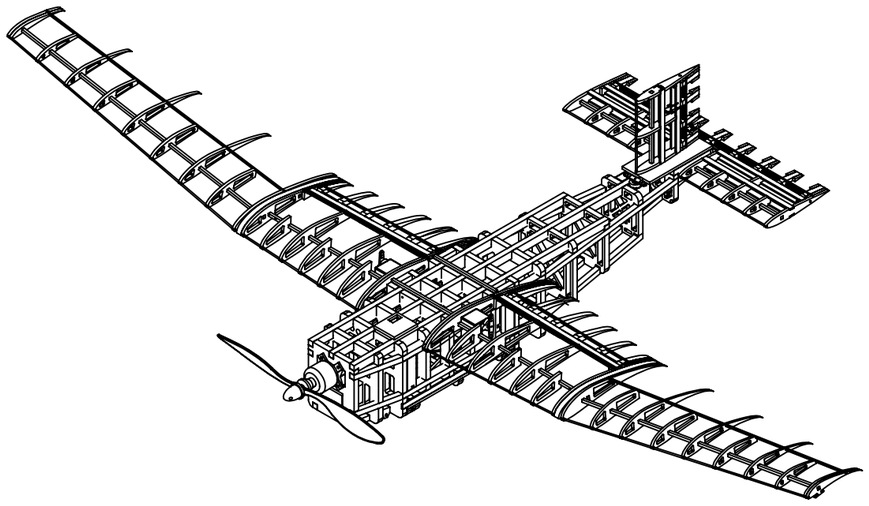

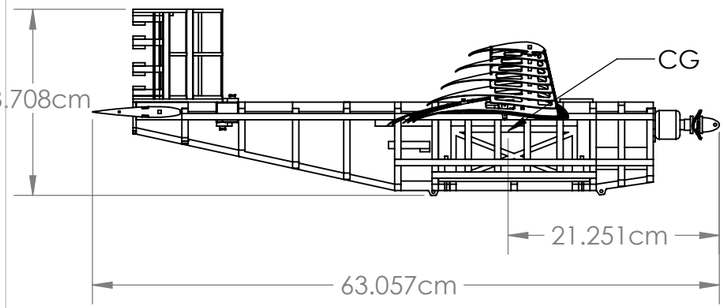

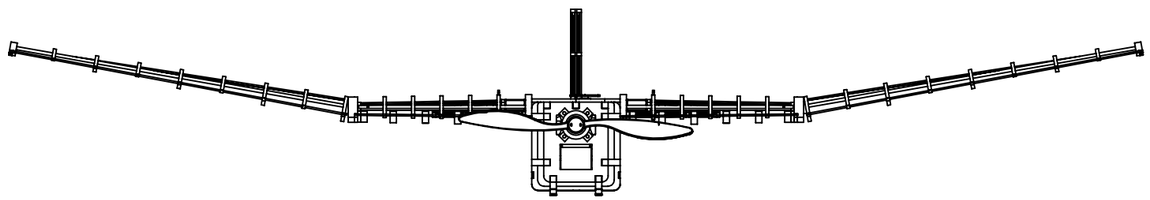

WORCESTER POLYTECHNIC INSTUTUTE
WPI HEAVY LIFT TEAM
TEAM 321
SHEET 1 OF 1

XFOIL was again used to find lift, drag, and moment coefficients of the S1223 at varying angles of attack. These values were graphed up to the stall point of the wing, and a linear fit was applied to the lift coefficient values. The slope of the line was used as the two-dimensional lift curve slope, $C_{l\alpha}$. The Mach number was computed using the velocity of the plane at cruise and the temperature of the air, and a specific heat ratio of 1.4, equation 3.6.

$$M = \frac{v}{\sqrt{\gamma R(Temp)}} \tag{3.6}$$

The leading edge sweep angle, the exposed planform area, and the body lifting factor were computed using the geometry of the wing (see Appendix B). Table 3.5 shows the results from the lift curve slope calculation:

Table 3.5 Wing Lift Curve Slope Results

$C_{l\alpha}$	5.798/rad
β	0.999
η	0.922
Λ_{LE}	0.052 rad
S_{exp}	0.134 m^2
$C_{L\alpha}$	**5.104/rad**

We also performed wind tunnel testing on our airfoil to obtain experimental data. The results below show the lift curve of the entire aircraft. For comparison, the lift curve slope of the scale model was 0.083/deg (4.756/rad), which is similar, but not equal to the wing lift curve slope (due to body and tail effects).

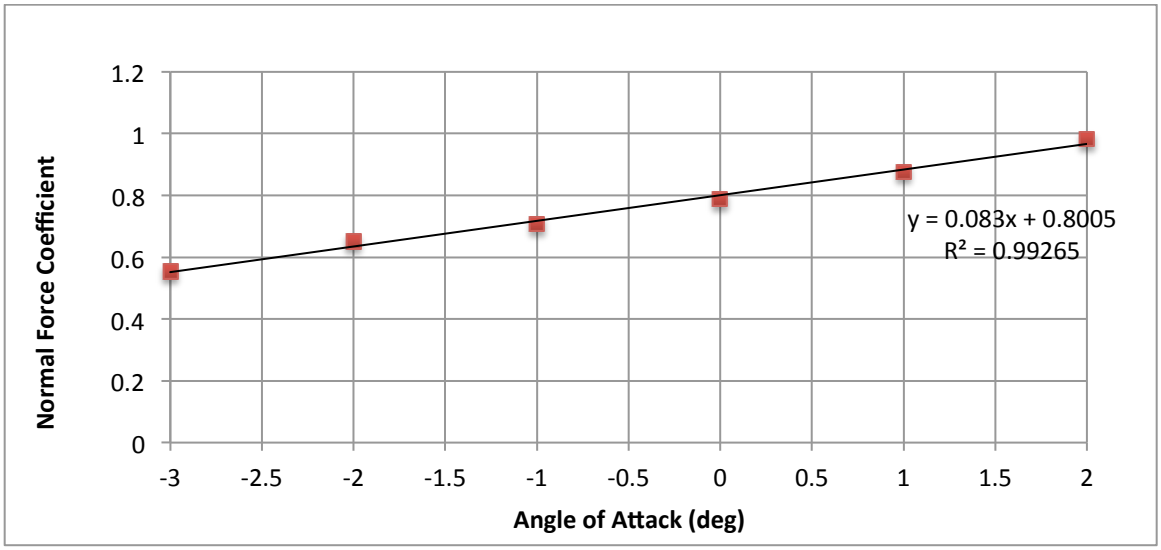

Figure 3.2 Normal Force Coefficient versus Angle of Attack of Scale Model

To find the lift curve slope of the tail, the same equations and procedure was used as for the wing. The XFOIL process for the NACA 0012 at appropriate Reynolds number yielded a two-dimensional lift curve slope of 6.37/rad. Using equation 3.5, with the geometric parameters of the tail, we computed a tail lift curve slope of 3.87/rad.

The aerodynamic center of the wing and tail was found using equation 3.7 [4].

$$\frac{x_{ac}}{\bar{c}} = -\frac{\partial C_{M,LE}}{\partial C_N} \tag{3.7}$$

With lift, drag, and quarter chord moment coefficient values from XFOIL, we could determine the normal force coefficient, equation 3.8 [3].

$$C_n = C_l \cos\alpha + C_d \sin\alpha \tag{3.8}$$

Equation 3.9 [3] allowed us to turn quarter chord moments into leading edge moments. Then, we applied 3.7, and took the average over the range of values.

$$C_{m,LE} = C_{m,c/4} - \frac{C_n}{4} \tag{3.9}$$

Thus, we found the wing aerodynamic center was at 23.27% of the chord and the horizontal tail aerodynamic center was at 27.16% of the chord.

3.5 Propulsion

The propulsion system was designed to produce the required thrust to overcome drag at cruise while weighing as little as possible. It was designed to operate for a minimum of two and a half minutes to accommodate for multiple circuits of the course at maximum speed plus a safety factor. The most important of these priorities was to produce enough power and, in turn, thrust to achieve flight.

To get an initial estimate of the power output needed, we used the rule of thumb of approximately 30 W per one lbf of weight lifted [9]. At the beginning of the design process, our initial weight was approximately five lbf and thus our required power was approximately 150 W.

Given the power estimate we determined a range of battery specifications that had the capability of producing a minimum of 150 W. In order to achieve this power output, batteries of different cell counts were considered. With the maximum voltage of two cell batteries set at 7.4 Volts, the maximum power output of a two cell battery was 133 W. As such, a three cell battery was chosen. Given the flight duration of two and a half minutes, a maximum amp-hour value for the battery was calculated to be 850 mAh at an operational current between 14A and 20A (burst current of 38.2 A) and battery specification voltage of 11.1V. With these values and assuming a flight current usage of 18 A, a power output of 199.8 W was calculated using the below equation:

$$P = I \cdot V \tag{3.10}$$

Next on the list of components to be chosen was the motor. With respect to the nature of power output of propeller motors and the inherent relationship between a motor and a propeller,

it was necessary to consider motor choice and propeller sizing in tandem. As such, the first general relation to consider was thrust versus RPM. Of course, higher RPM means higher thrust. Next to be considered was propeller pitch versus thrust. Consequently, lower pitches meant higher thrust values, but also lower RPM. Therefore, a higher power motor was required to spin a propeller with less pitch at the same RPM as one with more pitch. Finally, the relationship that brought the voltage of the battery and RPM of the motor together was the Kv parameter of the motor. Kv is a measure of the RPM per Volt a motor can output, and in doing so, how much torque a motor outputs. Lower Kv meant lower RPM with more thrust which was typical of slow flying planes, much like the very aircraft our team was designing [10]. Using these general guidelines as well as the parameters of the battery, the motor Kv value was selected to be 1200 Kv.

To determine prop size, it was necessary to relate thrust and power to pitch speed, V_{pitch}. Pitch speed can be calculated using equations 3.10 and 3.11:

$$RPM = K_v \cdot V_{battery} \tag{3.10}$$

$$V_{pitch} = RPM \cdot Pitch \cdot \eta_{\text{prop}} \tag{3.11}$$

From these equations, propeller diameter can be calculated using equation 3.12, 3.13 and 3.14 [10]:

$$T = \frac{P}{V_{pitch}} \tag{3.12}$$

$$A_{prop} = \frac{T}{(0.5 \cdot \rho \cdot V_e^2)} \tag{3.13}$$

$$D_{prop} = 2 \cdot \sqrt{\frac{A_{prop}}{\pi}} \tag{3.14}$$

Dynamic thrust had to be greater than static thrust. Since static thrust is dependent on the diameter of the propeller disk and the outgoing airspeed, we determined that a nine-inch diameter, 4.7 inch pitch propeller was needed for our application.

Table 3.6 Propulsion Summary

RPM	13320
Diameter x Pitch	9 x 4.7 in
Thrust	3.367 N
Thrust/Weight Ratio	0.165

3.6 Performance

To find an estimate for the drag of the aircraft, the design team used the drag buildup method, equation 3.15 [4]:

$$D_{total} = D_{induced,wing} + D_0 + D_{featheredprop} \tag{3.15}$$

This method involves breaking up the sources of drag into separate components: induced drag of the wing and parasitic drag of the wing, tail and body. An additional factor of feathered prop drag was added to simulate the drag of the propeller.

To find the induced drag of the wing, we used an estimate of the drag polar of the wing, equation 3.16 [4], where the Oswald efficiency factor is computed as shown.

$$C_{d,induced} = \frac{1}{\pi(AR)e}(C_l)^2 \tag{3.16}$$
$$e = 1.78(1 - 0.045(AR)^{0.68}) - 0.64$$

Thus, using XFOIL to find the lift coefficient at the desired angle of attack of the wing, the minimum drag coefficient of the wing, and the lift coefficient at minimum drag, we could apply equation 3.16. For the wing at cruise condition, we found a lift coefficient of 1.384, and an Oswald efficiency factor of 0.804. This yielded an induced drag coefficient of 0.092, or 0.961 N of drag exerted by the wing.

To find parasitic drag, we broke the plane down into four areas: the wing, the horizontal tail, the vertical tail, and the body, equation 3.17 [4].

$$C_{d0} = \frac{\sum_{c} C_{f,c} FF_c Q_c S_{wet,c}}{S_{ref}} \tag{3.17}$$

Thus for each component, we had to compute skin friction coefficients, form factor, component interference factor, and wetted surface areas.

For the wing, we used the flat-plate skin friction coefficient method. Using equations 3.18 [4], we found the laminar and turbulent skin friction coefficients, respectively, for the wing Reynolds number and Mach number.

$$\begin{aligned} C_{f,lam} &= 1.328/\sqrt{\mathrm{Re}} \\ C_{f,turb} &= \frac{0.455}{(\log_{10}\mathrm{Re})^{2.58} + (1+0.144M^2)^{0.65}} \end{aligned} \tag{3.18}$$

We used the average value of 0.006. We then found the form factor of the wing using equation 3.19.

$$FF = \left[1 + \frac{0.6}{(x/c)_m}\left(\frac{t}{c}\right) + 100\left(\frac{t}{c}\right)^4\right]\left[1.34M^{0.18}(\cos\Lambda_m)^{0.28}\right] \tag{3.19}$$

Using airfoil coordinates for the S1223, we found the thickest part of the airfoil was at 17.42% of the chord. At this location, the sweep of the wing was 0.016 rad (0.904°), and the thickness was 12.1% of the chord. These values allowed us to find a form factor of 1.035. Finally, we assumed a component interference factor of 1 in accordance with Raymer [4]. The wetted surface area was taken to be twice the planform area.

For the horizontal and vertical tails, we found an average skin friction coefficient of 0.007. The thickness of the NACA 0012 is 12%, located at 30% of the chord. Thus, we

computed a form factor of 0.908. As recommended by Raymer, a Q value of 1.05 was used [4]. The wetted surface area was taken to be twice the planform area.

For the body of the aircraft, the surface area of the body was determined using the external dimensions from Appendix A. Using the area of the empennage, and the sides and bottom of the body (since the wing covers the top side of the body), we computed a surface area of 0.163 m^2. The form factor was computed using equations 3.20 [4], with the maximum cross-section area of 0.008 m^2 (at the body section).

$$FF = \left(1 + \frac{60}{f^3} + \frac{f}{400}\right) \qquad f = \frac{l}{\sqrt{(4/\pi)A_{\max}}} \tag{3.20}$$

Using the length of the body as the characteristic length of the aircraft, we found a Reynolds number of 341548, and an average skin friction coefficient of 0.004.

Using equation 3.17, with the wing planform area taken to be the reference area, we found a parasitic drag coefficient of 0.006.

To find the feathered prop drag, we used equation 3.21 [4].

$$C_{D0,\,featheredprop} = 0.1\frac{n_{blades}}{\pi(AR)_{blade}}\frac{A_{prop}}{S_{ref}} \tag{3.21}$$

We took the propeller to have a diameter of nine inches and two blades with an aspect ratio of 6. Thus, we computed a feathered propeller drag coefficient of 0.152 N.

Summing up the above values, we found a total parasitic drag coefficient of 0.358, which, combined with induced drag, gave a total drag of 1.321 N at cruise. Drag force versus velocity is shown below, Figure 3.3. It is of note that the needed thrust for cruise is significantly less than

the maximum thrust of the propulsion system. This means that the aircraft can safely fly under the power of the motor.

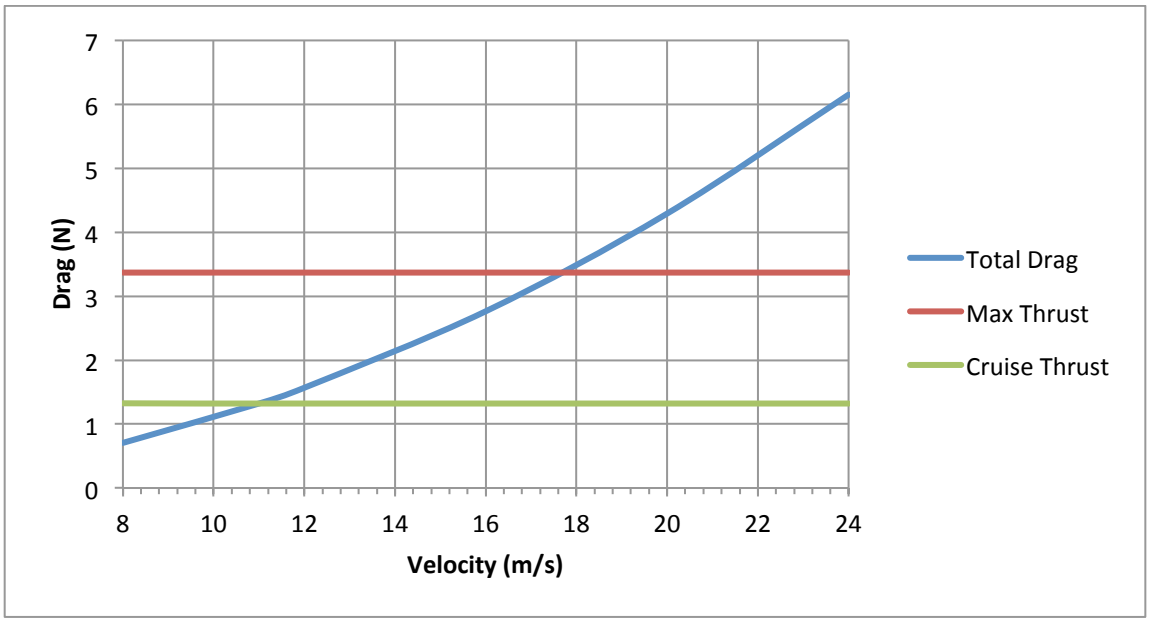

Figure 3.3. Drag Force and Thrust versus Velocity

3.7 Aircraft Stability and Control

3.7.1 Stability Analysis

Stability requires that the center of gravity (CG) be located ahead of the vehicle neutral point both with and without the payload. Since we used a space frame body, static pitch was our primary concern. The primary equations used to calculate the neutral point (np) and most forward point (mf) locations from the nose of the plane, and thus the stability envelope, are listed below, equations 3.22 and 3.23 [4].

$$\bar{x}_{np} = \frac{C_{L_\alpha,w}\bar{x}_{ac,w} + \eta_H \frac{S_H}{S} C_{L_\alpha,H} \frac{d\alpha_H}{d\alpha} \bar{x}_{ac,H}}{C_{L_\alpha,w} + \eta_H \frac{S_H}{S} C_{L_\alpha,H} \frac{d\alpha_H}{d\alpha}} \tag{3.22}$$

$$\bar{x}_{mf} = \frac{-0.15 + \bar{x}_{ac,w} + \eta_H \frac{S_H}{S} \frac{C_{L_\alpha,H}}{C_{L_\alpha,w}} \frac{d\alpha_H}{d\alpha} \bar{x}_{ac,H}}{1 + \eta_H \frac{S_H}{S} \frac{C_{L_\alpha,H}}{C_{L_\alpha,w}} \frac{d\alpha_H}{d\alpha}} \tag{3.23}$$

To minimize calculation error and expedite stability analysis an Excel worksheet was created. This worksheet held calculated flight coefficients, flight condition parameters, and plane dimensions. These values were used in the above equations to calculate the extent of our aircraft stability envelope. In addition to calculating the stability envelope, the worksheet was also created to estimate the CG location of our aircraft. The CG location was computed using the weight of components and estimated locations along the axis of the aircraft. This helped us determine preliminary positioning of the payload and electronics. As we completed our SolidWorks model, a more accurate estimate of the CG location was determined and compared to neutral and most-forward points. Table 3.7 shows the final stability calculations where the stability parameters are given as fractions of the mean aerodynamic chord.

Table 3.7 Longitudinal Stability Results

Stability Parameter	$Cl_{\alpha,w}$	$Cl_{\alpha,H}$	η_H	$\frac{d\alpha_H}{d\alpha}$	S_H/S	$\bar{x}_{ac,w}$	$\bar{x}_{ac,H}$	$\bar{x}_{np}$	$\bar{x}_{mf}$	$\bar{x}_{cg}$
Value	5.10	3.865	.9	.605	.177	0.833	3.508	1.015	0.875	0.974

3.7.2 Control Moment Analysis and Servo Sizing

In an effort to keep the plane as light as possible we minimized the weight of the servo based on the required torque, with a safety factor. By importing our airfoils into XFOIL, and taking advantage of the flap simulation feature, we were able to calculate the moment coefficient about the control surface hinge. Using the moment coefficient, density of air, flight speed and control surface dimensions, we calculated the hinge moment due to the aerodynamic forces. Combining this hinge moment with the gravitational moment due to the weight of the control

surface, we were able to calculate the overall hinge moments of the aileron and the elevator. Note that the weights of the control surfaces are including in the moment analysis. It was assumed that the servo for the elevator would be sufficiently powerful enough to actuate the rudder. The hinge moment data is tabulated in Table 3.8. With these hinge moments we found the lightest servos which could produce the required torques (which is, in fact, the smallest torqueing servos we could find).

$$H_{Total} = H_{Aerodynamic} + H_{weight} = C_{m,hinge}(.5\rho v^2 \bar{c} S_{control}) + W x_{cg,s} \quad (3.24)$$

Table 3.8 Control Surface Moments

Control Component	Span (cm)	Torque Required (kg-cm)	Servo Torque (kg-cm)
Ailerons	16.87	.378	1.296
Elevator	26.37	0.015	1.296

3.8 Structural Analysis

The most important element of structural analysis is wing loading. We estimated our wing loading by assuming our wing was a straight beam of uniform cross section (no polyhedral), and that the desired lift was spread over the wing in an elliptical loading. The loading on a half wing is shown below, Figure 3.4:

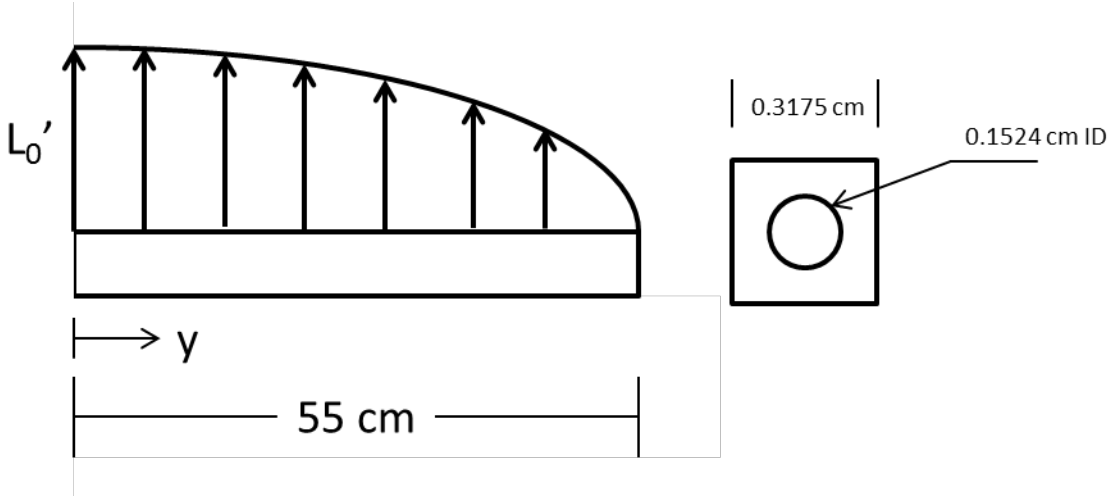

Figure 3.4 Beam Bending Free Body and Cross Section Diagram

The maximum stress in such a beam is at the wing root. Since our loading was assumed elliptical, we had to first compute the lift per unit span at the root of the wing. This was done by integrating the lift distribution and setting the value equal to half the desired weight of the plane, equation 3.25 [3].

$$\int_0^{b/2} L_0' \sqrt{1-(\frac{2y}{b})^2}\, dy = \frac{W}{2} \tag{3.25}$$

This gave a lift per unit span at the wing root of 17.57 N/m. We then computed the bending moment as a function of span wise (y) position, and found the moment at the wing root, equation 3.26 [3]:

$$M(y) = -M_{root} + \int_0^y s L_0' \sqrt{1-(\frac{2s}{b})^2}\, ds \tag{3.26}$$

At the wing root, the bending moment was -5.925 N-cm. For the given cross section (see Figure 3.4 above), we computed the area moment of inertia, equation 3.27:

$$I_{zz} = I_{zz,square} - I_{zz,circle} = \frac{l_{side}^4}{12} - \frac{\pi}{4} r_{hole}^4 = 8.204 \cdot 10^{-4}\, cm^4 \tag{3.27}$$

We computed the maximum bending stress, which occurred at either the top or bottom of the cross section, using equation 3.28:

$$\sigma_{\max} = \frac{M_{root} \cdot (l_{side}/2)}{I_{zz}} \tag{3.28}$$

The computed maximum stress was 1146.5 N/cm^2 or 11.465 MPa, which is lower than the yield strength of the carbon fiber spar, approximately 1740 to 2170 MPa [11].

4. Innovations

4.1 Glider Construction

First, we decided to build a glider in order to familiarize ourselves with designing and constructing a model aircraft. This exercise made us aware of the considerations that have to be taken into account to ensure that the aircraft flies and that it can be assembled in the short time frame allowed for the competition. By building the glider we discovered how challenging designing our aircraft was when accounting for the competition rules. We realized then that we would need a three-piece wing to produce the necessary amount of lift for our aircraft.

Constructing a glider allowed us to observe the effect that different wing and tail configurations had on the performance of the aircraft. Also by constructing a glider, we got to practice the design principles to quickly construct an inexpensive aircraft. By doing this we would hopefully avoid some mistakes when constructing our actual plane for the competition.

While testing our plane we discovered another challenge posed by the rules. By requiring aircraft to be hand launched we were faced with the challenge of getting our aircraft to be thrown at a fast enough speed that would prevent it from crashing to the ground as soon as it was released. Also we had to design the body of the plane to be structurally sound enough to withstand being gripped tightly when being thrown. The glider was thrown several times. We noticed that the best results occurred when the glider was thrown up at an angle. We therefore realized that in order to get the best lift generation, our wings should be mounted at angle of attack greater than zero. The glider also flew best when the tail was in line with the wing (versus located below the wing).

From constructing the glider our lessons learnt were:

- Mount wings at angle of attack greater than zero degrees

- Multiple piece wing
- Body needs to be sturdy
- S1223 difficult to construct

4.2 Rapid Prototyping and Wind Tunnel Testing

Our next innovative technique was to create scaled three-dimensional models of our aircraft using our university's rapid prototyping (RP) machine. By using this rapid prototyping method we were able to have models with various configurations to test in WPI's 2'x2' wind tunnel. Unlike constructing a glider, rapid prototyping was not a time-intensive task. We simply had to construct a SolidWorks model and send it off to the printer. However since the RP machine can only use certain material, our models produced did not have the same weight or weight distribution as our actual aircraft. Therefore we could only use the three-dimensional models produced through rapid prototype for lift and drag tests in the wind tunnel but not for actual flight testing or stability analysis.

4.3 Balsa Wood Construction and Mylar Application

We manufactured parts using aero grade balsa wood in addition to regular grade balsa. We found the aero grade balsa to be far too fragile for the aircraft and decided not to use it. We also applied a thin sheet of fiberglass using resin to the longerons experiencing significant stresses due to the wing spar. When applying the Mylar, several hands were required to maintain the profile of the airfoil. We attempted to apply the Mylar using Balsarite and using the base adhesive, and the base adhesive proved sufficient for the application. Regular super glue was used in construction to shorten construction time with negligible change in weight [12]. In every structural failure case, the balsa split before the glue separated. This will be particularly useful in

the event of damage to the aircraft during the competition. The addition of tabs to our design also expedited the construction process, another competition friendly decision.

4.4 Laser Cut Parts

The ability to laser cut every part of the aircraft, whether it was Mylar, balsa, or acrylic proved an invaluable innovation in the construction process. As expected, during construction parts are frequently damaged. Being laser cut allowed us to quickly make parts and spares for the construction process. It also allowed us to design complex geometries that would otherwise be impossible to manufacture. The laser cut acrylic landing gear was lighter, cheaper, and just as capable as purchased alternatives, while being fully customizable. Laser cut Mylar supports allowed for weight saving cutouts to be placed in the thinnest components of the aircraft, while still providing Mylar application support. In addition, laser cutting the supports allowed for us to mimic the desired geometry accurately over multiple parts. This result was key to having balanced wings

5. Fabrication

5.1 Overview

Over the course of the project, several iterations of the aircraft were constructed. Each one allowed us to test and evaluate the feasibility of the design and practice different construction techniques. One complete glider and two powered aircraft were constructed in addition to several practice subassemblies. For powered aircraft, a bill of materials and construction plan was written to facilitate the process. Below are several of the major phases in the construction process.

5.2 Laser Cutting

Before construction began, the balsa sheet components of the aircraft were cut using the laser cutter. Standard process for the VLS laser printer was to model all parts in drafting software, produce a drawing with only the outlines of the part, and export that drawing to AutoCAD. These parts were printed from AutoCAD. For the final model of the aircraft, the laser cutter was also used to cut thick Mylar precisely. The key challenges to using the laser cutter were determining proper settings for each thickness of wood and providing tolerance to structurally significant cutouts. Mock printing sessions were used prior to cutting plane parts in order to discover optimal printing settings for different job types. Balsa wood and Mylar are soft materials so they cut at a faster speed then the harder, more common acrylic materials that the laser cutter is usually used for. For each build session the cutting process took approximately an hour.

5.3 Assembling and Covering Components

After the balsa and Mylar parts were cut and each part was accounted for the next step was to assemble plane components in the following order:

- Horizontal Stabilizer
- Vertical Stabilizer
- Elevator
- Rudder
- Fuselage and Empennage
- Central Wings
- Ailerons
- Wing Tips
- Payload Carrier
- Landing Gear

This order allowed us to prioritize the construction of components such that there was smooth integration into the final product. A small group would focus on assembly, then hand the completed part over to a second group to apply Mylar, and then off to another group to assemble.

To have a successful build required some coordination. A clutter-free construction area in Higgins 216 was created so that builders could focus more on building procedure and less worrying about lab accidents. The tools used for construction were also given assigned locations so that any builder could easily find them. A disposable drop cloth was placed over a table to ensure spills of Balsarite, lacquer, glue, or any chemicals used would not harm the table and be easy to clean up.

For joining balsa and Mylar pieces we used Impact Strength Instant Gorilla Glue at all junctions. Instant Gorilla glue dried rapidly with minimal expansion, which allowed assemblies to be constructed quickly. We used a precision knife and box cutter to cut the basswood, balsa wood, and carbon fiber spars to size. Often, we sanded spars and holes of parts to ensure that

pieces fit well without the need of extraneous force. Toothpicks were used to get glue into smaller spaces. A construction tooling was used in order to guarantee that ribs were positioned and oriented accurately.

It was necessary to construct the tail section of the plane first because, in the final construction of the plane, the tail added support at the end of the empennage. To construct the stabilizers we started off with a basswood spar that was cut to span wise length of the stabilizer. Next a series of airfoil ribs were precisely positioned along the spar using the help of the construction tooling. Before the glue dried fully, the leading and trailing edge balsa wood rounds and Mylar-supporting balsa sheets were glued into place along the rib surfaces. After the glue dried the construction tooling was removed and the component was placed away from the build table where it waited to be covered with Mylar.

After the stabilizers were finished we then constructed the respective control surfaces. The rudder and elevator, like the stabilizers, were constructed in a similar manner. We started by adding small Mylar support wedges to both sides of the trailing edges of the control surface ribs. Next we positioned the ribs into our construction tooling and glued balsa wood spars into the inserts on the upper and lower surfaces of the ribs. We made sure to overcut the spar each time when constructing all control surfaces, because adding end caps after applying Mylar helped the fit of the parts from catching during actuation.

The next section constructed was the fuselage. The construction procedure for the fuselage was designed to be as simple as possible. The rib-longeron design made assembly of the parts similar to a jigsaw puzzle. Once constructed, the parts were glued in place. Some parts needed to be left open for electronics integration. To facilitate electronics integration, cutouts were designed into the ribs for running wiring and placing components.

Construction of the wing was broken into three parts: central wing sections, ailerons, and wing tips. The central wings were constructed first and had a similar construction procedure to that of the stabilizers. The wings, however, required more effort and attention to detail because they had more different parts and needed to be of nearly perfect condition and orientation for successful operation. The wing differed from the stabilizers in that the primary spar was carbon fiber, that it had to detach from the plane, and the airfoil used was cambered. The carbon fiber rod was first cut to size and drilled with a $1/16^{th}$ inch bit to fit a connecting pin that joined the wings. The basswood secondary spar was cut and sanded. Then the ribs, Mylar supports, and edge spars were added just like the stabilizers.

The ailerons were built using the same procedure as the rudder and elevator. However, in addition to the standard balsa parts the ailerons received thick Mylar sheets along the bottom surface of their trailing edges. These thicker strips allowed for better definition of the trailing edge of the airfoil during Mylar application. The Mylar support strengthened the trailing edges while also creating a well-defined trailing edge, which prevented the upper and lower Mylar surfaces from touching.

The wing tips were essentially just an extension of the central wing that needed to include a 10 degree angle. To achieve a proper 10 degree angle a protractor was used to establish a reference angle. This was usually drawn directly onto the table cloth. Two basswood spars were then joined together at a 10 degree angle. Like the ailerons, a piece of thick Mylar was applied to the trailing edge of the wing tip. The wing tips like the control surfaces had cap ribs that were applied after sealing. The cap ribs for the wing tips allowed for attachment of a tensioned nylon string without interrupting the covering Mylar of the wing.

After each component was constructed they were next sealed with Mylar. The specifics of this process are outlined in Section 5.5. Mylar covering was an important part of the process and followed the construction of every plane component barring those that needed to be open for electronics integration.

The final components constructed were the landing gear and payload carrier. The payload carrier was simply a box and just needed to be assembled and sealed with Mylar since its bottom was also part of the fuselage. The landing gear was constructed from a piece of acrylic, laser cut and bent to shape using a blowtorch. A thin axle ran through the frame, attaching the wheels and rubber stops.

5.4 Final Assembly and Electronics Integration

Gluing the larger structural components of the plane together had to be done in a certain order. The horizontal stabilizer was first attached to the body, and vertical stabilizer was put in place. The wing tips were attached to the central wings. Control surfaces were hinged using a carbon fiber rod, which was glued into place. Finally, the landing gear attached to the body and the nylon tension string was attached to the wing tips.

During this step in the process, electronics were integrated into the body. Special care was taken to ensure correct orientation and fit of electronic components. This required cutting wires to proper length, and mounting the servos, motor, speed controller and receiver. By running the wires through holes in the ribs of the body, we ensured that the wiring was neat and easy to follow without interfering with the payload. All electronics were mounted using glue except the battery which needed to be removable.

After the electronics were integrated and the plane was completely sealed electronics were checked for flight readiness. The build process took two days to complete.

5.5 Mylar Application Guide

Mylar is an excellent choice for covering the wing because it is very light and resistant and to tears. However, the application of Mylar took effort and literature on proper techniques was not easy to find. We experimented with using airplane dope for Mylar adhesion, but we found it was unnecessary in terms of time and added seal.

We used 0.00025 inch thick Mylar based on recommendations. Mylar has a matte side, which contains the adhesive, and a reflective side. Mylar is heat activated so a heating iron was required. The process for applying Mylar is detailed below:

1. We cut a piece of Mylar that was slightly larger than the area trying to be covered.
2. We aligned the grains of the Mylar to run in the span-wise direction of the part being covered (this was particularly important for the wings and tail).
3. We used the heating iron to seal the Mylar to the structure, making sure to keep it as taut as possible.
4. After the part has been completely covered with Mylar, we ran the heating iron over the cells in the direction of the Mylar grains to tighten it. Slow, unidirectional strokes worked best.

If airplane dope was being used, the following steps had to be taken before Mylar was applied:

1. The airplane dope was diluted with lacquer thinner.
2. It was then brushed lightly to cover the part.
3. We left the part to dry for about two minutes, then proceeded to cover as outlined above.

6. Results

6.1 Wind Tunnel Test

Two scale models of the aircraft were made using the rapid prototyping machine. These were mounted on the HL 216 force balance and placed in the wind tunnel in the basement of Higgins Labs. The first prototype constructed was 1:4 scale to fit the 2 ft by 2 ft test section of the wind tunnel. The following data was acquired during testing of the 1:4 scale model, Table 6.1.

Table 6.1 1:4 Scale Model Test Results

Angle of Attack (degrees)	Normal Force (N)	Axial Force (N)	Pitching Moment (N-m)
0	7.34	0.31	0.694
3	9.34	-0.80	0.868

The data showed values which were less than expected. We attribute these discrepancies to scaling effects and the difficulties associated with prototyping small and intricate geometries.

Because of the printer's limitations for printing thin parts (specifically the trailing edge of the S1223), a second, 3:8 scale model was prototyped. This model incorporated additional features to ensure the accuracy of the model. Unfortunately, the results still left much to be desired. Again, we attribute these discrepancies to similar causes as in the first test. Figure 6.1 below shows the results for the 3:8 scale model.

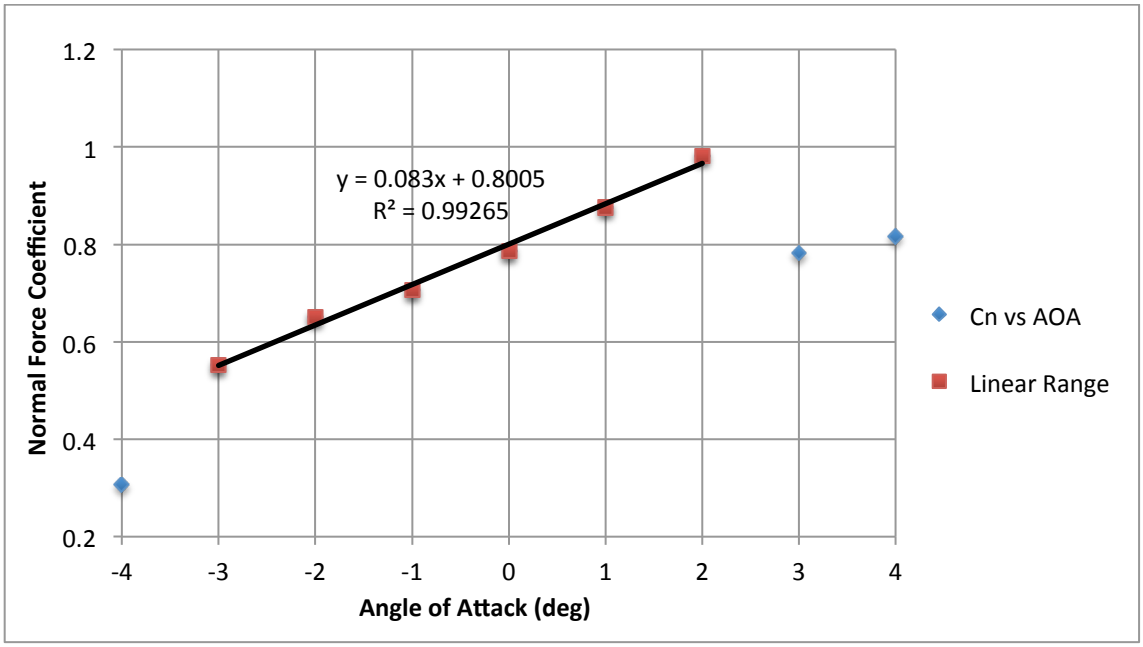

Figure 6.1. Normal Force Coefficient versus Angle of Attack for 3:8 Scale Model

Figure 6.1 shows the normal force coefficient as a function of angle of attack of the model. For angles between -3 and 2 degrees, the model exhibited a linear trend. However, beyond 2 degrees, the wings started fluttering, which we attribute to stalling at the wing tips due to improper geometry. This data shows a lift curve slope of 0.083/deg (4.756/rad), which is still less than expected.

6.2 Glide Test

With the successful construction of an unpowered Iteration 4 prototype, we were able to test the glide ratio of the aircraft. Weighing down the nose of the aircraft to provide longitudinal stability, we hand launched the aircraft in an indoor environment. The result of the glide test was a glide ratio of approximately 8. This value is similar to the 10.76 glide ratio expected using the lift and drag coefficients from analysis. We expected the tested glide ratio to be less than computed because, in order not to damage the prototype, we caught it mid-glide.

6.3 Wing Break Test

A simple wing loading test was performed on the prototype to determine the strength of the wings. Using batteries as weights, we distributed the load over both wings to simulate in-flight loading. The aircraft failed at a distributed load of 12.75 N. This value was slightly less than required. Inspection of the failure showed fracture along the grain of the $1/8^{th}$ inch panels of the body. This showed that the wings themselves were strong enough and that the body needed redesign.

6.4 Flight Test

Several attempts at flight were made with the flight worthy iterations of the aircraft. Ultimately, only iteration 5 flew successfully. Iteration 4 suffered a structural failure along the grain of the balsa frame. Iteration 5 flew successfully two times without payload before the motor sustained damage. While a replacement motor was selected, the motor did not meet the exact specifications of the design motor. The replacement motor had a Kv value of 1020 as opposed to the original value of 1200, and weighed 87g vs 47g. We were unable to achieve sustained flight with the replacement motor. Upon re-examination of the propulsion equations it was discovered that the motors selected provided less thrust with higher torque than the original motor. A larger propeller was necessary to provide equivalent thrust with replacement motor as was provided by the initial motor.. The nature of prop motors makes it difficult to determine dynamic thrust values of the propulsion system. The initial motor provided adequate static thrust to power the aircraft. However, static thrust data on the replacement motor was not collected in the interest of time.

7. Summary

As forms the basis of the Aero East competition, we designed an airplane to carry the maximum possible payload while weighing the least within the competition constraints. By setting the bar as high as possible, we accounted for major modifications along the way and maintained our competitive edge despite problems with the initial design. Our final product is designed to carry 12.6 N while weighing 4.4 N. This yields a payload fraction of 74%. It is designed to withstand the rigors of multiple flights in moderate wind conditions. It is also designed to be a forgiving aircraft to fly, having control surfaces that are less sensitive than a regular aircraft's. Finally, the aircraft is designed to be easily put together at the competition, in line with the three minute limitation.

We built several aircraft during the course of this project. We successfully flew our aircraft twice without payload. Ultimately our plane was unable to lift the desired payload because the selected motors did not provide sufficient thrust to achieve sustained flight while carrying payload. With additional time and budget we would have purchased the appropriate motor.

Overall, the project provided an excellent experience in group dynamics, resource management, and aircraft design. We hope that the endeavors of this project will benefit future MQPs to come.

8. Recommendations

This section is written in such a way to give directions to those who might benefit from this information.

8.1 Overall

Aircraft Design (ME 4711) provides information critical to the success of this project. It outlines the aircraft design process, and explains the step-by-step nature of the process more in-depth. Because we had not taken this class, we left to figure out the process on our own. This meant that certain portions of the analysis were performed out of order or in ways that were not appropriate. Therefore, we recommend that ME4711 be taken in Junior year or A-Term of Senior year to provide students with the necessary knowledge to successfully design an aircraft. Being familiar with the material would also help the group to keep pace with the recommended timeline for the project.

Identify which members are strongest at computer aided design (CAD). This project is very involved using programs such as SolidWorks and AutoCAD. CAD is important for designing the aircraft, obtaining aircraft stability margins, and creating layouts for part construction. Having multiple group members capable of modeling expedites the process of turning design sketches into an actual model.

Make use of file sharing tools such as Dropbox. Organization is very important in keeping track of progress and prevention of file and document loss. Having materials consistently available to *all group members* in their most current form allows for everyone to work on their own time rather than needing the whole group together to accomplish tasks.

8.2 Design

Have a solid understanding of the rules of the competition, most importantly the eligibility of materials. Knowing whether or not you can use materials such as fiber reinforced plastics can save time spent on redesigning and lead times waiting for materials to arrive.

In the early stages of designing the aircraft, follow the aircraft design process. Most flight characteristics are dependent on others, requiring you to choose certain specifications to obtain others. However, following the aircraft design process early on will prevent "running in circles" while determining initial specifications.

When choosing a fuselage configuration, a rib-longeron construction is much stronger than a space frame construction. This helps to mitigate the structural weakness of thin wood sheets which tend to split along the grain. It is important to over-design for structural strength rather than to under-design for weight savings.

Weight estimates for the aircraft will be off. Wood will not always be identical, electronics will be heavier than you expect, and other miscellaneous construction materials will build up. Wiring for electronics can amount to substantial weight, not to be dismissed without thought. Mylar and glue will also contribute more weight than expected.

8.3 Testing

Testing using scale models may not produce accurate data based on trends and expected values obtained through analysis of full-scale design. Results obtained through wind tunnel and force balance testing often returned values lower than those expected. Wind tunnel testing is useful in observing stall characteristics of the wing profile, particularly those of varying geometry and dihedral/polyhedral angle.

In testing the flight capability of powered models, we recommend to takeoff from the ground first, before attempting a hand-launch. It is important to trim control surfaces before taking flight, and the need to trim can be observed from how the aircraft rolls during ground takeoff. Flight testing with no weight or a small percentage of the desired payload is suggested to check for aircraft stability.

Choosing a testing environment is as important as the testing itself. Determine if testing conditions are suitable for your aircraft. Gusts of wind can have devastating effects on Micro Air Vehicles (MAVs). Choose an area with appropriate landing conditions. The surface should be appropriate for the aircraft's chosen landing mechanism, whether they are skids or wheels. Snow can be an effective and safe landing surface so long as the top is not iced over.

Expect multiple failures during testing. As extensive as preparations may be, there will be something which is overlooked or underestimated which will cause a failure within the plane, whether it is catastrophic or minor. Make sure to leave sufficient time for multiple builds and tests.

8.4 Construction

Aircraft sizing will not be as exact as in a computer model. Adding tolerances to tight fitting parts is advised as laser cut pieces of wood will not always exactly match that which it is designed for. However, we found that sanding pieces down to size can also be effective and prevent the need of creating brand new parts.

Expect difficulties using the laser cutting machine. The process of laser cutting parts can be tedious on its own even when the laser cutter is working efficiently. In laying out the parts on sheet sized drawings, ensure that the parts are fitted closely together to maximize the use of the wood, but allow enough of a buffer on the edges as to prevent the cutoff of important parts.

Laser cutting can also be finicky in requiring particular settings for different thicknesses of wood, not necessarily those given by default for that thickness. Without the right settings, the wood may catch fire or split, rendering several parts or even an entire sheet unusable.

Buy more material than you require. In aircraft such as these, parts are small and fragile. Parts are bound to break and having spares will save a week's worth of time waiting for new parts to come in. The use of quick-drying superglue is suggested to minimize downtime while sections of the plane need to dry before the addition of adjacent parts.

Have a construction plan before attempting to construct the aircraft. Know which parts need to connect to which in order to prioritize which parts need to be constructed first. The use of construction tooling, especially in the construction of the wings, tail, and control surfaces can be very useful in ensuring symmetry and proper spacing.

Landing gear can be made lightweight, inexpensive, and strong using the laser cutter. A piece of acrylic can be cut using the laser cutter, and bent into shape using a blow torch.

References

[1] SAE. "SAE Collegiate Design Series: Aero Design: About Aero Design." *Student Central.* Web. 05 Dec. 2011. <http://students.sae.org/competitions/aerodesign/about.htm>

[2] SAE. "2012 Collegiate Design Series: Aero Design East and West Rules." *Student Central*. Web. 05 Dec. 2011. <http://students.sae.org/competitions/aerodesign/rules/rules.pdf>.

[3] David J. Olinger, ME 4770 Student Notes, Unpublished

[4] Raymer, D. P., ed. (2006). *Aircraft Design: A Conceptual Approach 4th Edition.* Virginia: AIAA.

[5] SAE. "2011 Micro Class Results." *Student Central*. Web. 5 Dec. 2011. <http://students.sae.org/competitions/aerodesign/east/results/2011micro.pdf>.

[6] Homs A., McGrath S., Micallef A., Ryan S., Zatorski Z., *SAE Aero Design Competition Heavy Lift Cargo Plane Micro Class.* Engineering Design and Prototyping Report, Stevens Institute of Technology.

[7] Selig, Michael S. "High-Lift Low Reynolds Number Airfoil Design". Published in *Journal of Aircraft*, Vol 34, No. 1, January-February 1997.

[8] "S1223." *Airfoil Investigation Database*. Web. 28 Feb. 2012. <http://www.worldofkrauss.com/foils/1421>.

[9] Design Guidelines for Electric Powered Motors". *MaxCim Motors, Inc.* Web. 07 Dec 2011. http://www.maxcim.com/guide.html

[10] "Electric Motors for Model Aircraft".Web 07 Oct 2011. http://adamone.rchomepage.com/guide5.htm

[11] CES EduPack 2011 (Version 7) [Software]. (2011). Cambridge, UK: Granta Design.

[12] MSDS – Gorilla Glue Products. http://www.gorillaglue.com/information/MSDS.aspx

Appendix A. Payload Prediction Graph

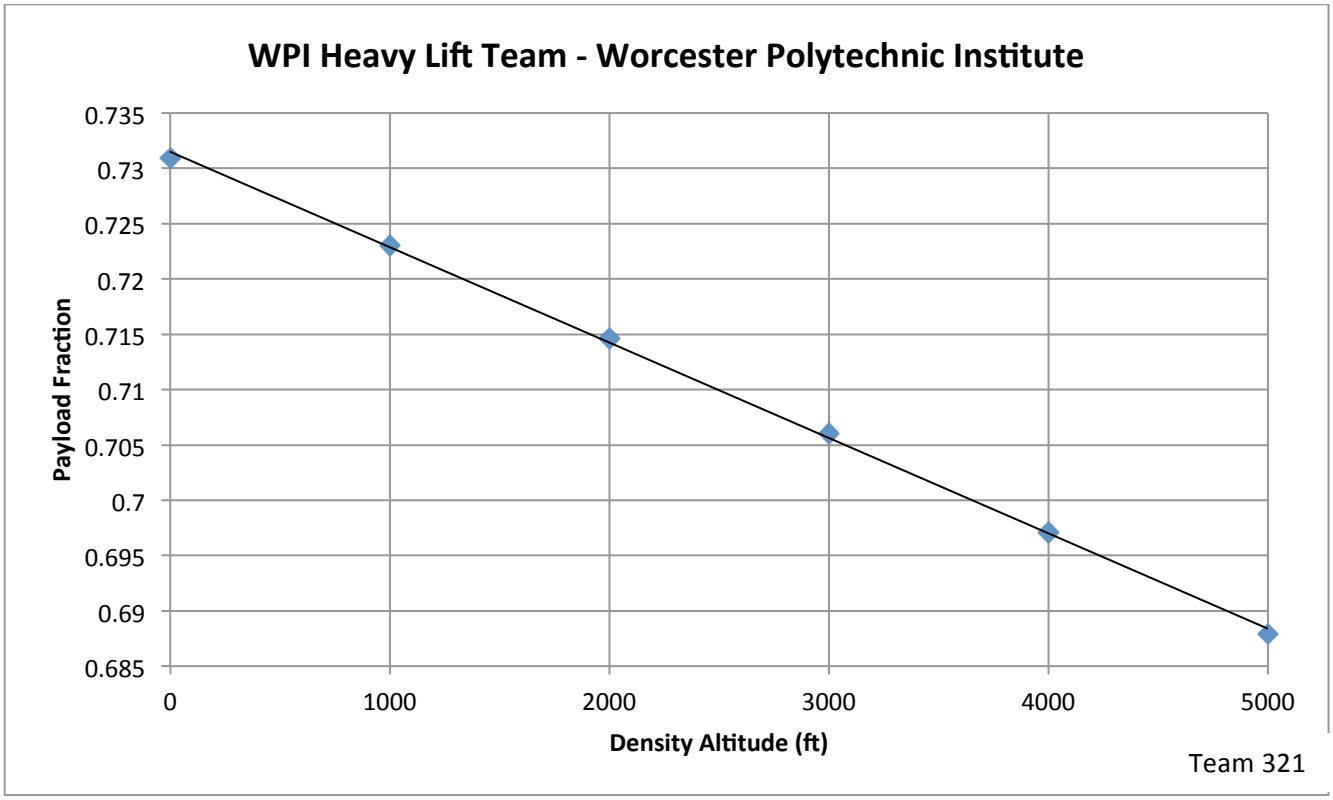

Figure A.1 Payload Prediction Graph

$$PF = (-9 \cdot 10^{-6})h + 0.7315$$

WINGSPAN	114 cm
HEIGHT	18.7 cm
LENGTH	63.1 cm
WING AREA	f
ENGINE	eRC 400 Brushless
EMPTY WEIGHT	1 lbf

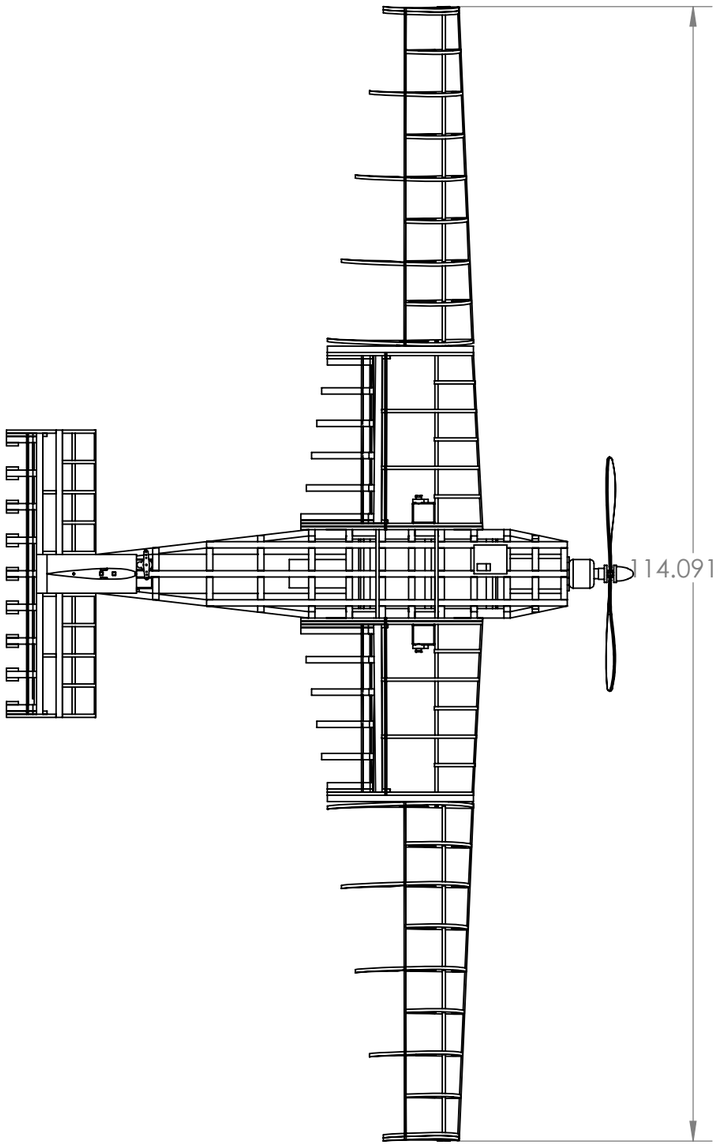

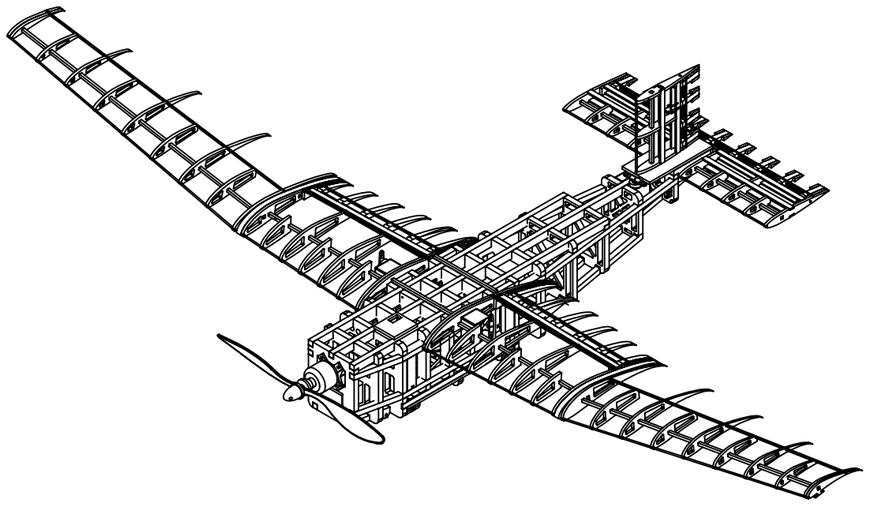

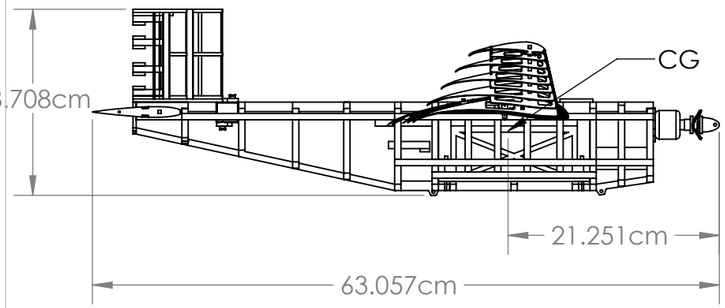

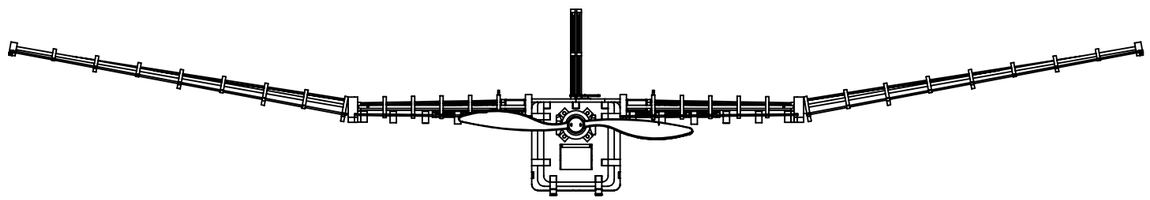

WORCESTER POLYTECHNIC INSTUTUTE
WPI HEAVY LIFT TEAM
TEAM 321
SHEET 1 OF 1